Available online at www.sciencedirect.com
ScienceDirect
Journal of Sound and Vibration 322 (2009) 241–254
JOURNAL OF SOUND AND VIBRATION
www.elsevier.com/locate/jsvi

The influence of cross-order terms in interface mobilities for structure-borne sound source characterization: Force-order distribution

H.A. Bonhoff*, B.A.T. Petersson

Institute for Fluid Mechanics and Engineering Acoustics, Technical University of Berlin, Einsteinufer 25, 10587 Berlin, Germany

Received 9 September 2008; received in revised form 11 November 2008; accepted 12 November 2008
Handling Editor: M.P. Cartmell
Available online 6 January 2009

Abstract

For the characterization of structure-borne sound sources with multi-point or continuous interfaces, the concept of source descriptor and coupling function can be reformulated by incorporating the interface mobilities. The applicability of this approach, however, depends on the admissibility of neglecting the so-called cross-order terms. Hence, the objective of the present work is to investigate the importance and significance of cross-order terms for the characterization of vibrational sources. Such cross-order terms consist of the previously studied cross-order interface mobilities and the force orders which are addressed herein. The distribution of force orders depends on both the complex data of the contact forces and their location along the interface. From measurements and numerical simulations it is found that the relative magnitudes of the force orders vary up to a factor 10. Only at low frequencies a larger range in magnitude can be observed. Combined with the knowledge of the cross-order interface mobilities, henceforth, a complete assessment of the influence of cross-order terms is possible.

1. Introduction

For the characterization of vibrational sources and the description of the transmission process of source–receiver assemblies, the source descriptor and coupling function were introduced [1]. The application for multi-point and continuous interface systems is possible by incorporating the concept of interface mobilities [2]. With the concept of interface mobilities, the physical source is subdivided into a series of theoretical source orders. In order to allow the individual source orders to be treated as single-point and single-component systems, the cross-coupling between different orders has to be neglected. The so-called cross-order terms describe this cross-coupling and consist of force orders and cross-order interface mobilities.

In some cases, the distribution of the force orders can be pivotal for the admissibility of neglecting the cross-order terms. Consider the case where a force order p is substantially smaller than another force order q and the

*Corresponding author. Tel.: +49 30 31428996; fax: +49 30 31425135.
E-mail address: hannes.bonhoff@tu-berlin.de (H.A. Bonhoff).

0022-460X/$ - see front matter © 2008 Elsevier Ltd. All rights reserved.
doi:10.1016/j.jsv.2008.11.030

Nomenclature

Symbols

C	interface circumference
f	frequency
F	force
$\hat{F}_q$	force order
k_q	interface number
M	number of sampling points
N	number of contact points
p, q	order numbers
s_0	interface coordinate
Y	mobility
$\hat{Y}_{pq}$	interface mobility
$\hat{Y}_{p-p}$	equal-order interface mobility
α	angle between contact points

Indices

L	order number of the force order with the smallest magnitude within a confidence interval
U	order number of the force order with the largest magnitude within a confidence interval

cross-order interface mobility $\hat{Y}_{p-q}$ is of similar magnitude as the equal-order interface mobility $\hat{Y}_{p-p}$. Here, the equal-order approximation is likely to give a poor estimate of the source descriptor and coupling function of order p, see Ref. [2]. This is due to the fact that the cross-order term $\hat{Y}_{p-q}\hat{F}_q$ is larger than the equal-order term $\hat{Y}_{p-p}\hat{F}_p$.

If all force orders are approximately equal, the cross-order terms reduce to the cross-order interface mobilities. In this case, therefore, the importance of the cross-order interface mobilities applies for the validity of the equal-order approximation.

In recent work [2,3], the influence of cross-order interface mobilities has been investigated for a variety of generic structures. In this work, solely the distribution of the force orders is studied with a view towards a complete assessment of the significance of the cross-order terms. Whilst it is recognized that moment excitation can be significant [4], the analysis is limited to forces perpendicular to the structure. The theoretical background and the fundamental definitions as well as the field of application associated with the concept of interface mobilities for the present study are the same as those presented in Ref. [2].

2. Force orders

For source–receiver assemblies incorporating multiple contact points, a single closed-contour interface of circumference C can be considered, which passes all contact points, see Fig. 1. With N point forces along the

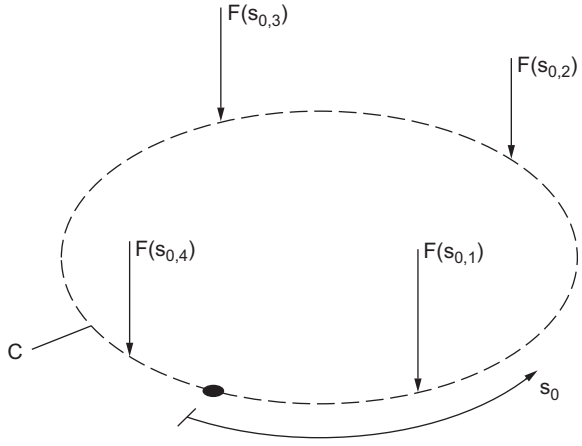

Fig. 1. Schematic illustration of a source–receiver interface passing four contact points. --- Interface; • origin of the interface coordinate.

interface, a continuous spatial force distribution can be described by

$$F(s_0) = \sum_{n=1}^{N} F(s_{0,n})\delta(s_0 - s_{0,n}). \tag{1}$$

A list of symbols is given in the Nomenclature. The force distribution along the interface can be series expanded by means of a spatial Fourier decomposition

$$F(s_0) = \sum_{q=-\infty}^{\infty} \hat{F}_q(k_q)\mathrm{e}^{\mathrm{j}k_q s_0}, \quad k_q = \frac{2q\pi}{C}, \quad q \in \mathbb{Z}, \tag{2}$$

with the force orders defined as

$$\hat{F}_q(k_q) = \frac{1}{C}\int_0^C F(s_0)\mathrm{e}^{-\mathrm{j}k_q s_0}\,\mathrm{d}s_0. \tag{3}$$

The force orders $\hat{F}_q$ can be interpreted as the complex amplitudes of waves travelling along the interface. The exponential terms in Eq. (2), $\mathrm{e}^{\mathrm{j}k_q s_0}$, describe the initial spatial distribution of such waves as illustrated in Fig. 2. Combined with the force orders, these spatial distributions are adjusted in accordance with the actual forces at the contact points. The force-order magnitude scales the distribution in amplitude, while the phase of the force orders results in a shift along the interface.

Upon substituting Eq. (1) into Eq. (3), the force orders for an interface with N point contacts are obtained as

$$\hat{F}_q = \frac{1}{C}\sum_{n=1}^{N} F(s_{0,n})\,\mathrm{e}^{-\mathrm{j}k_q s_{0,n}}. \tag{4}$$

If the contact between the source and the receiver is continuous or partially continuous, the Dirac Delta function is inappropriate for the calculation of the spatial force distribution. In such cases, a linear interpolation can be assumed between the sampling or measurement points [5]. For an interface discretized at M points, the zero-order and qth-order forces can be derived from Eq. (3) as

$$\hat{F}_0 = \frac{1}{2C}\sum_{m=1}^{M}\{(s_{0,m} - s_{0,m-1})[F(s_{0,m}) + F(s_{0,m-1})]\} \tag{5}$$

and

$$\hat{F}_q = \frac{j}{k_q C}\sum_{m=1}^{M}\left[F(s_{0,m})\mathrm{e}^{-\mathrm{j}k_q s_{0,m}} - F(s_{0,m-1})\mathrm{e}^{-\mathrm{j}k_q s_{0,m-1}} - \frac{F(s_{0,m}) - F(s_{0,m-1})}{\mathrm{j}k_q(s_{0,m-1} - s_{0,m})}(\mathrm{e}^{-\mathrm{j}k_q s_{0,m}} - \mathrm{e}^{-\mathrm{j}k_q s_{0,m-1}})\right], \tag{6}$$

respectively. If the sampling points are distributed with equal distance along the interface, a fast Fourier transform algorithm can be employed for the calculation of the force orders.

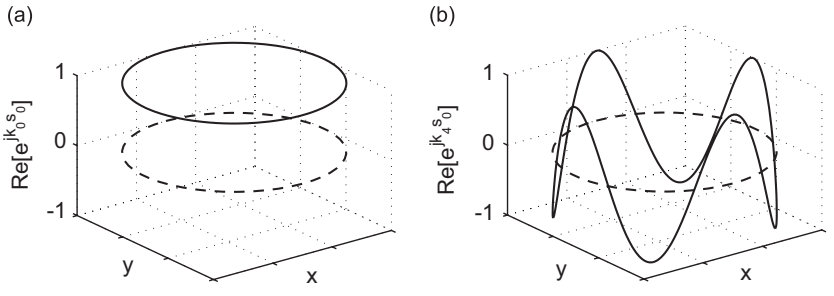

Fig. 2. Schematic illustration of the spatial distribution of two force orders over a circular line interface: (a) zero order; (b) fourth order. — Spatial distribution; - - - interface.

3. Basic force-order distributions

The distribution of the force orders depends on both the relative magnitudes and phases of the forces at the contact points. The phases of the force orders additionally depend on the location of the origin of the interface coordinate s_0 and are not considered in this study. In the following, the force-order distributions are exemplified through generic cases of a four-point source–receiver installation with equi-distant spacing between the contact points.

In Fig. 3, the force-order dependence on the magnitude of the contact forces is illustrated. Two examples of spatial force distributions with the resultant force orders are presented. Fig. 3(a) shows the case where the contact forces are in phase and of equal magnitude at all contact points. Such a spatial force distribution can be approximated by the sum of the force orders presented in Fig. 2. For an exact reproduction, the forces of order 0, ±4, ±8, $\pm12,\ldots$ have to be equal in magnitude, while all other orders vanish, see Fig. 3(a).

Removing one contact point and letting the other three contact forces remain equal in magnitude and phase, results in the spatial force distribution in Fig. 3(b). In the resultant force-order distribution, the orders which were zero in the previous configuration, are now present and of equal magnitude. Furthermore, the forces of order 0, ±4, ±8, $\pm12,\ldots$ still are dominant. Hence, the two force-order distributions in Fig. 3 show a high degree of similarity.

In Fig. 4, the force-order dependence on the phase of the contact forces is illustrated. Two examples of spatial forces and force-order distributions are plotted. The magnitudes of the contact forces are equal, while they are either in phase or out of phase. When comparing Figs. 4(a), (b) as well as Fig. 3, it can be seen that the force-order distributions differ markedly. All force orders which are present in one case are equal to zero in the other two cases.

Based on comparisons such as those presented in Figs. 3 and 4, it can be concluded that the dependence of the force orders on the phase of the contact forces is larger than on the relative magnitudes. Variations in the phase of the forces at the contact points can lead to completely different distributions of force orders. Changes in the magnitudes result in far less distinct variations of the force-order distributions.

In Figs. 3 and 4, a grouping of the force orders is observed. Clusters of four force orders, starting with order zero, are repeated in the interface order domain. For an interface with N contact points, which are distributed with equal distance along the interface, it can be stated that $\hat{F}_q = \hat{F}_{q\pm N}$. With an equi-distant spacing between

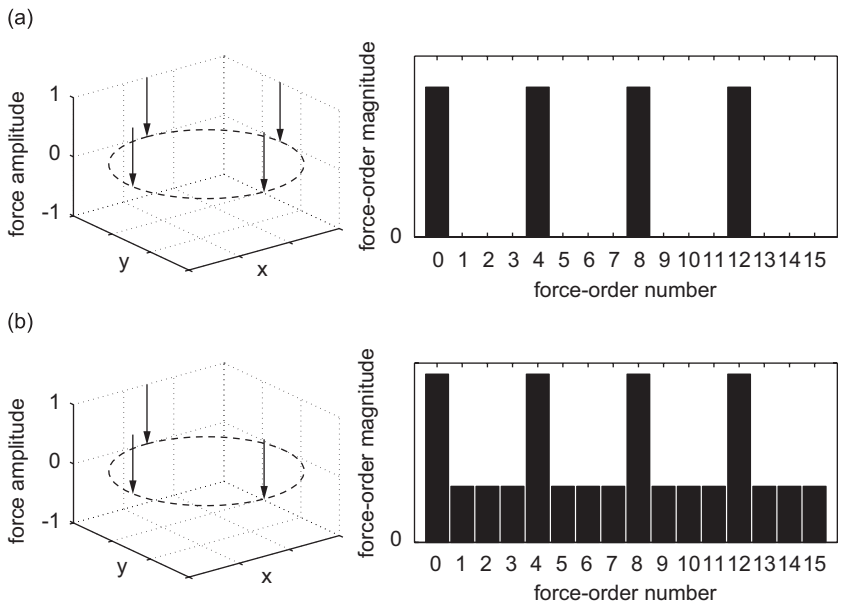

Fig. 3. Example of the force-order dependence on the relative magnitudes of the forces at the contact points. ⟶ Force at contact point; --- interface.

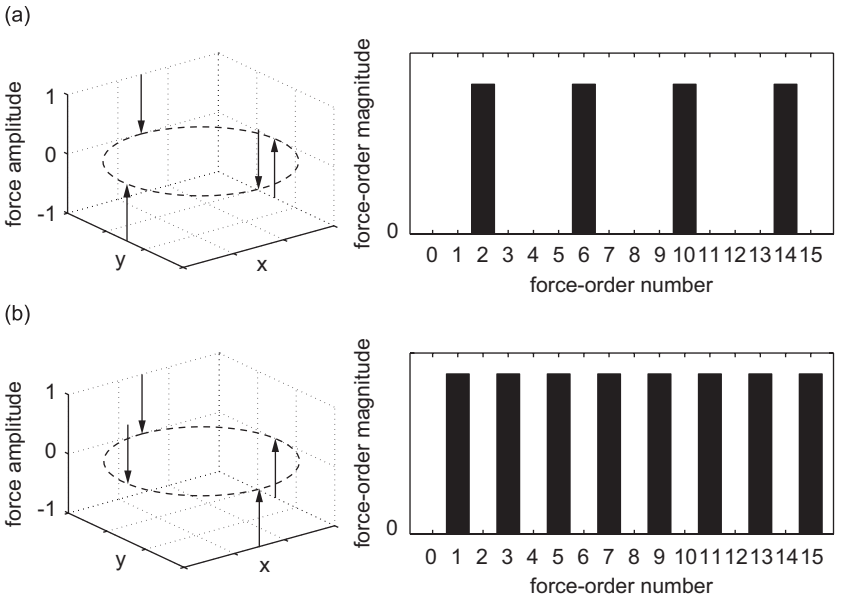

Fig. 4. Example of the force-order dependence on the relative phases of the forces at the contact points. ⟶ Force at contact point; - - - interface.

the contact points and the origin of the interface coordinate located at $s_{0,N}$, see Fig. 1, Eq. (4) can be rewritten as

$$\hat{F}_q = \frac{1}{C}\sum_{n=1}^{N} F\left(\frac{nC}{N}\right) \mathrm{e}^{-\mathrm{j}2n\pi q/N} \tag{7}$$

and

$$\hat{F}_{q\pm N} = \frac{1}{C}\sum_{n=1}^{N} F\left(\frac{nC}{N}\right) \mathrm{e}^{-\mathrm{j}2n\pi((q/N)\pm 1)}. \tag{8}$$

Owing to the periodicity of the complex exponential terms, Eqs. (7) and (8) are equal. However, if the contact points are not equi-distant spaced along the interface, the grouping will break up as shown in Section 5.

4. Force-order distributions of a tumble dryer and a washing machine

For the investigation of the distribution of force orders at source–receiver interfaces in practice, a tumble dryer and a washing machine have been examined. The washing machine was spinning at 600 rev/min and therefore represents a tonal source, while the tumble dryer behaves more as a broad-band source. The forces at the contact points were measured by placing the machine on force transducers. Both machines were measured empty in order to include only source mechanisms of the machine components and not of the water or textiles. Furthermore, the vibrations of the washing machine with a larger unbalanced mass might become nonlinear. Since there was no laundry present and nothing was changed during the various measurements, the repeatability for both machines was high. For these measurements, it was assured that the background noise was at least one order of magnitude below the measured signal. The machine footings are treated as point contacts, such that Eq. (4) is applicable for the calculation of the force orders.

In Fig. 5, the locations of the contact points along the circular interface are presented for both machines. The bold solid line between the points $s_{0,1}$ and $s_{0,2}$ indicates the front of a machine. As can be seen from Fig. 5, the spacing between the contact points is not constant for either of the machines. Hence, the grouping of the force orders is expected to be less pronounced than for the interface of the previous section. Although not

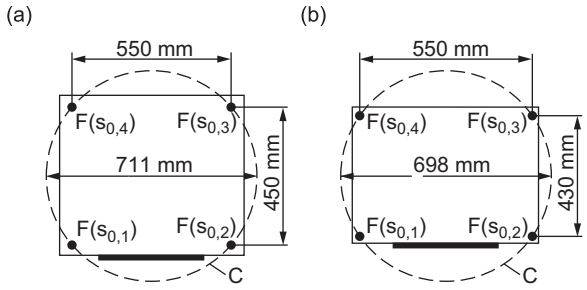

Fig. 5. Positions of the contact points of the machines along the circular interface: (a) tumble dryer; (b) washing machine. — Machine body; - - - interface; • contact point.

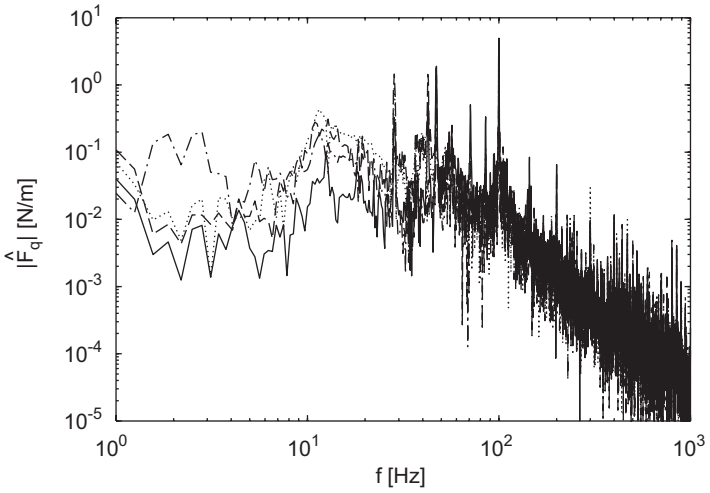

Fig. 6. Force-order spectra for a tumble dryer on a concrete floor. — $\hat{F}_0$; – – – $\hat{F}_1$; – · – $\hat{F}_2$; ····· $\hat{F}_3$.

explicitly shown, the first four force orders manage to capture the overall trends of the distribution in magnitude of all orders.

4.1. Tumble dryer

In a first measurement setup, the forces at the contact points were recorded with the tumble dryer standing on a concrete floor. The magnitudes of the first four force orders obtained from Eq. (4) are plotted in Fig. 6.

At frequencies above about 10 Hz, the magnitudes of all force orders lie within a band with a width of approximately one order of magnitude. Below 10 Hz, variations of up to two orders of magnitude can be observed. The narrow peaks in magnitude, such as that at 100 Hz, are found for all orders. Due to the logarithmic scale, the peaks and troughs are not distinguishable at high frequencies. Hence, the range in magnitude of the force orders in Fig. 6 in the upper frequency region appears larger than the actual maximum force-order ratio 10. Single force orders which dominate or are substantially smaller than all other orders at certain frequency regions are not found.

In a second setup, the tumble dryer was placed on a chipboard plate of 18 mm thickness, supported by two wooden joists, see Fig. 7(a). One side of the machine was located on a joist and the other side on a bay. The contact points at $s_{0,1}$ and $s_{0,4}$ therefore experience a different receiver mobility than the remaining two points, see Fig. 5(a). Furthermore, the vibratory behavior of the chipboard plate differs from that of the uniform concrete floor. Hence, both the relative magnitudes and phase of the contact forces are changed from those exerted at the concrete floor receiver.

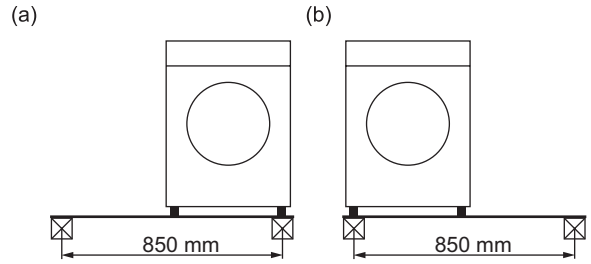

Fig. 7. Measurement setup for the investigation of the force-order dependence on the relative magnitudes and phase of the contact forces: (a) tumble dryer; (b) washing machine.

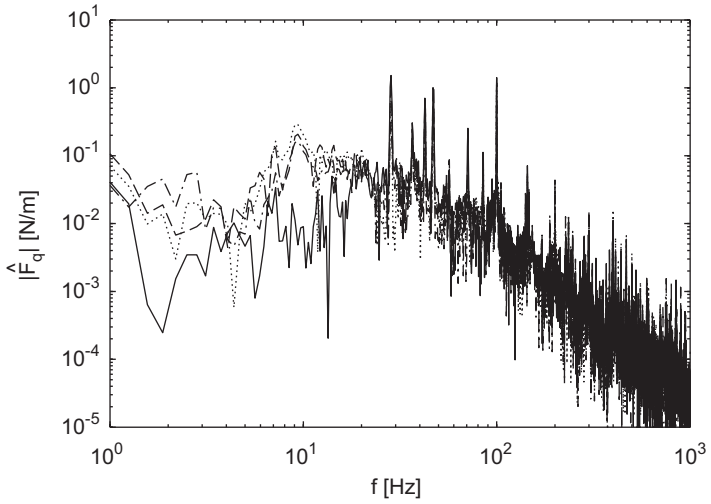

Fig. 8. Force-order spectra for a tumble dryer on a chipboard plate. — $\hat{F}_0$; – – – $\hat{F}_1$; – · – $\hat{F}_2$; ····· $\hat{F}_3$.

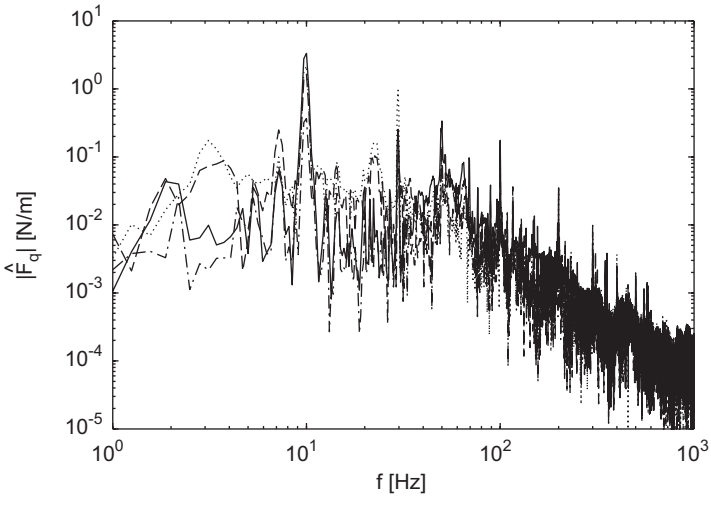

Fig. 9. Force-order spectra for a washing machine spinning at 600 rev/min on a concrete floor. — $\hat{F}_0$; – – – $\hat{F}_1$; – · – $\hat{F}_2$; ····· $\hat{F}_3$.

The lowest four force-order spectra are plotted in Fig. 8 for the tumble dryer on the chipboard plate. At frequencies below 20 Hz, the influence of the zero-order force is smaller than for the case of the concrete floor receiver. Between 20 and 50 Hz, the difference in magnitude between the orders has decreased. In an overall

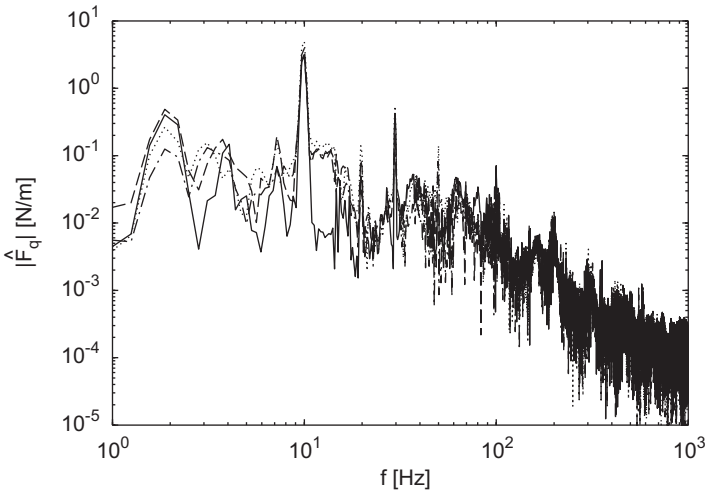

Fig. 10. Force-order spectra for a washing machine spinning at 600 rev/min on a chipboard plate. — $\hat{F}_0$; – – – $\hat{F}_1$; – · – $\hat{F}_2$; ····· $\hat{F}_3$.

sense, the same dependencies are observed as for the case of the concrete floor receiver. Only the frequency is shifted to approximately 20 Hz below which force-order ratios of up to 100 are observed.

4.2. Washing machine

For the washing machine installed on a concrete floor, the four lowest force-order spectra are plotted in Fig. 9. As the washing machine is spinning at 600 rev/min, a dominating peak is found at 10 Hz. At that frequency, the zero-order force is largest in magnitude. At frequencies in the vicinity of 10 Hz, a grouping can be observed between even and odd orders of forces. In these frequency regions, the even orders are of lower magnitude than the odd orders, similar to the theoretical case shown in Fig. 4(b). At frequencies above around 50 Hz, all force orders lie within a band of width of approximately one order of magnitude. Below 50 Hz, force-order ratios of up to 100 can be found. As for the tumble dryer, single force orders which dominate or are substantially smaller than all other orders at certain frequency regions do not exist.

In another set-up, the washing machine is installed on a chipboard plate as shown in Fig. 7(b). One side is located on a joist, while the other side is between two joists. Hence, the contact points at $s_{0,2}$ and $s_{0,3}$ experience a different receiver mobility than the other two, see Fig. 5(b). With the additional change in the vibratory behavior of the receiving structure, both the relative magnitudes and phases of the contact forces differ from the previous installation on the concrete floor.

In Fig. 10, the four lowest force-order spectra are plotted for the washing machine standing on the chipboard plate. The zero-order force is no longer the strongest order at the spin frequency and the grouping of even and odd force orders has vanished. Except for a few frequencies, the force-order ratios do not exceed an approximate value 10 in the entire frequency range under consideration.

5. Simulations of force-order distributions

The forces at the contact points of source–receiver installations have previously been investigated in conjunction with effective mobilities [6]. In Ref. [6], the assumption of equal magnitude of the contact forces was introduced. In an experimental investigation [7], it was found that the force magnitudes vary by a factor up to 100 at low frequencies but converge with increasing frequency. From the measurements of a washing machine and a tumble dryer, the variations between the magnitudes of the contact forces were observed to range up to a factor 10 in the entire frequency region [8].

The relative phases of the forces at four-point source–receiver interfaces have been analyzed by Fulford and Gibbs [9–11]. The contact forces can be obtained from the three variables, source free velocity and source and

receiver mobility [12]. The phase of the mobility or the free velocity of e.g. a resonance-controlled source can assume any value between $\pm\pi$. Furthermore, the phase will fluctuate in this frequency region and can therefore be described as random. It is argued in Ref. [11] that the relative phases of the contact forces are random within a certain frequency band if the phase of at least one of the former three variables is random. Where the phases of mobilities and free velocities are deterministic and the internal excitations of the source are coherent, the contact forces will either be in phase or out of phase [10,11].

In the following, the effect of random and deterministic relative phases of the contact forces on the distribution of force orders will be discussed.

5.1. Random phase of the contact forces

At frequencies where the source is stiffness or resonance controlled, the phases of the contact forces can assume any value between $\pm\pi$, see Ref. [11]. As there are infinitely many possibilities, Monte Carlo simulations [13] are suitable in order to gain information about the statistical properties of the resulting magnitude distributions of the force orders. Supported by an assumption in Statistical Energy Analysis [14], a uniform distribution of the phase is suggested in Ref. [11]. With the same argument, a uniform distribution is applied in the following analysis.

A typical magnitude distribution of the force orders for an interface with four contact points and equi-distant spacing is presented in Fig. 11(a). Plotted are 20,000 force orders ($\hat{F}_0$, $\hat{F}_{\pm1}$, $\hat{F}_{\pm2}, \ldots$) which were calculated with Eq. (4). The forces at the contact points have unit magnitude and random phase between $\pm\pi$. As discussed in Section 3, the force orders are stacked in four groups. In order to provide information about the range in magnitude of the force orders, the maximum force-order ratio can be calculated, i.e. $|\hat{F}_U|/|\hat{F}_L|$, see Fig. 11. Hence, the maximum force-order ratio relates to the 100% confidence interval.

In a first Monte Carlo simulation, 100,000 force-order distributions were calculated, where the four equi-distant contact forces have unit magnitude and random phase. The distribution of the resultant force-order

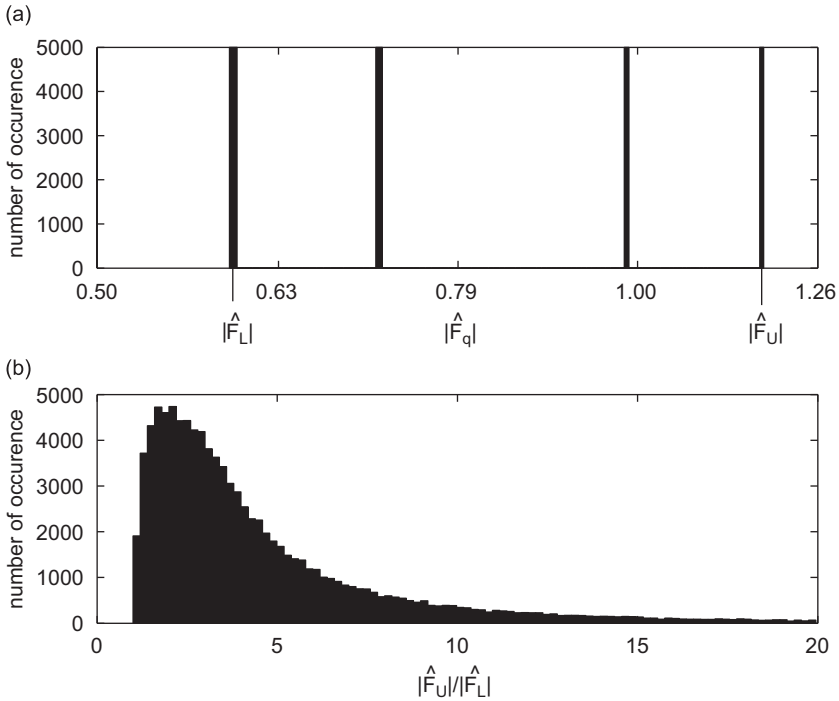

Fig. 11. Magnitude distribution of force orders for an interface with four equi-distant spaced contact points with unit magnitude and random phase between $\pm\pi$: (a) distribution of 20,000 force orders ($\hat{F}_0$, $\hat{F}_{\pm1}$, $\hat{F}_{\pm2}, \ldots$) with indication of the 100% confidence interval; (b) distribution of the force-order ratios for the 100% confidence interval.

Table 1
Median force-order ratios corresponding to the 100% confidence interval for interfaces with equi-distant spacing between the contact points.

Number of contact points, N	2	3	4	5	6	7	8	9
Random phase within interval $\pm\pi$, unit magnitude	2.4	2.4	3.5	4.2	4.7	5.2	5.6	6.1
Random phase within interval $\pm\pi$, random magnitude within 0.9–1.0	2.4	2.4	3.5	4.2	4.7	5.2	5.6	6.1
Random phase within interval $\pm\pi$, random magnitude within 0.5–1.0	2.3	2.5	3.4	4.1	4.6	5.1	5.6	6.1
Random phase within interval $\pm\pi$, random magnitude within 0.0–1.0	1.5	2.6	3.2	3.8	4.4	4.9	5.4	5.8

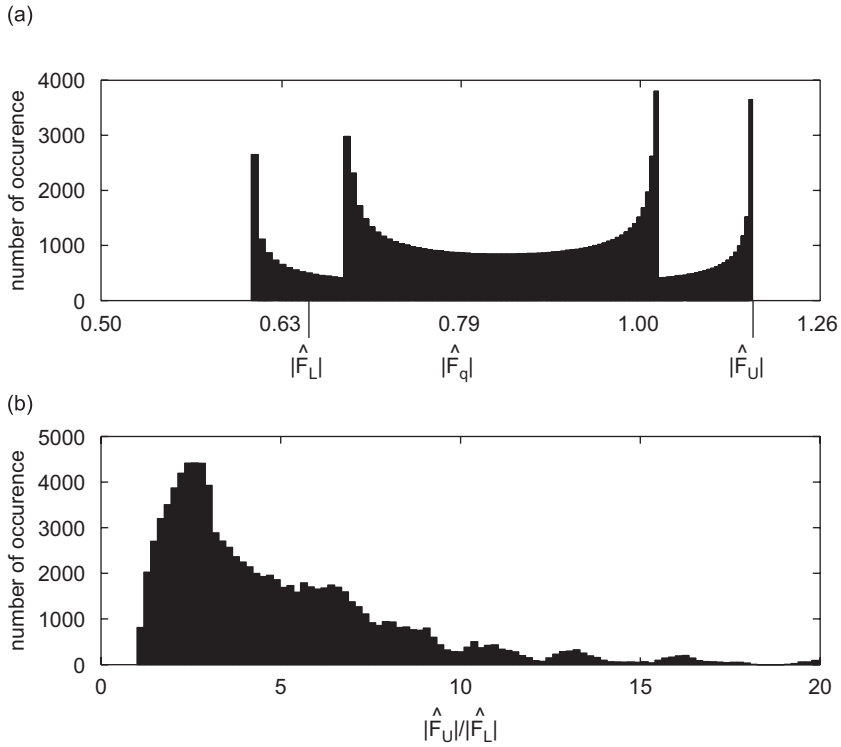

Fig. 12. Magnitude distribution of force orders for the interface geometry of a washing machine, see Fig. 5(b), with contact forces of unit magnitude and random phase between $\pm\pi$: (a) distribution of 100,000 force orders ($\hat{F}_0$, $\hat{F}_{\pm1}$, $\hat{F}_{\pm2}$, ...) with indication of the 90% confidence interval; (b) distribution of the force-order ratios for the 90% confidence interval.

ratios for the 100% confidence interval is shown in Fig. 11(b). Naturally, a force-order ratio relating to a certain confidence interval has a minimum of unity. As there are cases where certain force orders are equal to zero, see Figs. 3 and 4, maximum values of infinity are possible. One sample out of a population of force-order ratios which is equal to infinity is sufficient to yield a mean value of infinity. Hence, the median value of the distribution of force-order ratios corresponding to a certain confidence interval is a more useful measure of the average [15].

In Table 1, the median force-order ratios corresponding to the 100% confidence interval are listed for interfaces with equi-distant spacing between the contact points. Since $\hat{F}_q = \hat{F}_{q+N}$, see Section 3, only N force orders have to be calculated with Eq. (4) in order to obtain the force-order ratios. Every median force-order ratio in Table 1 is taken from a population of 100,000 force-order ratios. The values of both magnitude and phase of the contact forces are distributed with uniform probability within the specified intervals.

As seen in Table 1, the median force-order ratio increases with the number of contact points and thereby with the number of force orders which are different in magnitude. Varying the magnitude of the contact forces additional to the phase results in minor changes of the median force-order ratios presented in Table 1.

If the contact points are not equally spaced along the interface, the grouping of the force orders will brake up. In Fig. 12(a), an example of a magnitude distribution of force orders is plotted for the interface geometry of the washing machine, see Fig. 5(b). Plotted are 100,000 force orders ($\hat{F}_0$, $\hat{F}_{\pm1}$, $\hat{F}_{\pm2}$, ...) with the contact forces having random phase and unit magnitude. With such a distribution, a 90% confidence interval can be calculated as indicated by the upper and lower bounds $|\hat{F}_U|$ and $|\hat{F}_L|$. From a simulation of 100,000 force-order distributions such as that shown in Fig. 12(a), the force-order ratios corresponding to the 90% confidence intervals are plotted in Fig. 12(b).

In a next set of Monte Carlo simulations, the range in magnitude of the force orders is investigated in dependence of the spatial distribution of the contact forces. The analysis is limited to four-point interfaces with rectangular alignment of the contact points. As shown in Fig. 13(a), α is defined as the angle between two contact points along the interface. An angle of $\alpha = 90^\circ$, therefore, results in an equi-distant spacing between the contact points. For every angle α, 100,000 force-order distributions such as that presented in Fig. 12(a) were calculated.

In Figs. 13(b) and (c), the median force-order ratios for different confidence intervals are plotted for interface geometries with α ranging from 1° to 90°. For the case with random magnitude of the contact forces, the force orders vary slightly more than for the case with unit magnitude. However, both cases are approximately equal in an overall sense. On average, the force orders vary by a factor of approximately 4 for the 90% confidence intervals. For the 100% confidence intervals, the median force-order ratios are smaller than 10 for all values of α.

At angles of 90°, 60° and 45°, the three curves in Figs. 13(b) and (c) coincide. Such values of α correspond to interfaces with 4, 6 and 8 equi-distant contact points, respectively, where the additional forces are equal to zero. If there are less than 10 different force-order magnitudes, the confidence intervals for 100%, 95% and 90% are equal. The curve for the 100% confidence interval is seen to have distinct minima at angles where the contact points have equal spacing. As is observed in conjunction with Table 1, the 100% confidence interval tends to increase with the number of force orders which are different in magnitude.

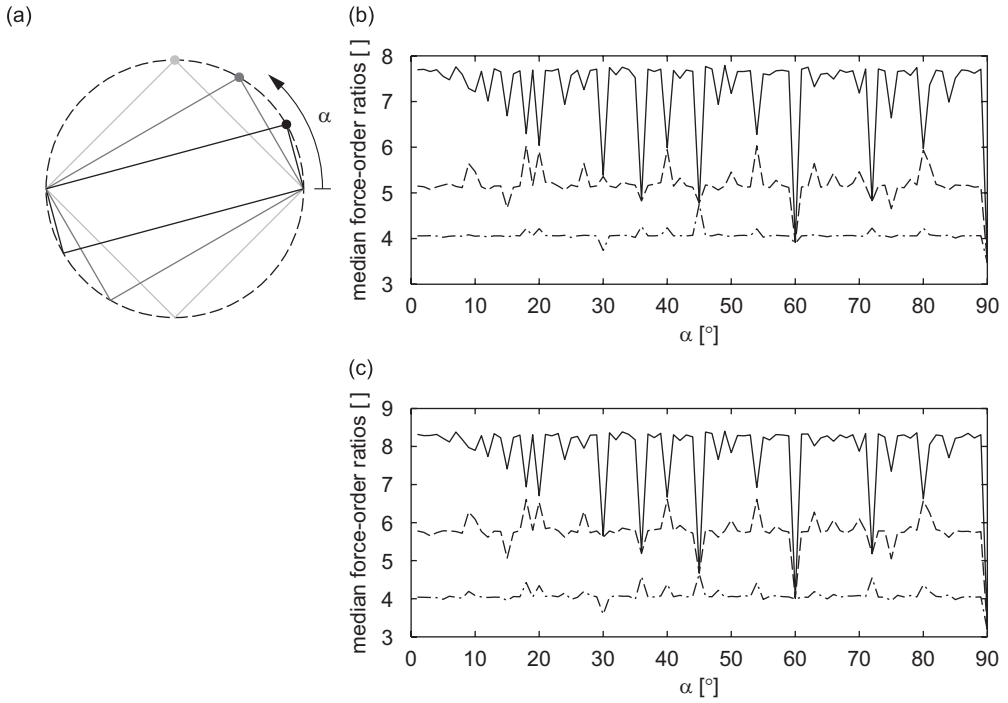

Fig. 13. Median force-order ratios in dependence of the spatial distribution of the contact forces: (a) definition of the angle α; (b) unit magnitude and random phase; (c) random magnitude and random phase. — 100% confidence interval; – – – 95% confidence interval; – · – 90% confidence interval.

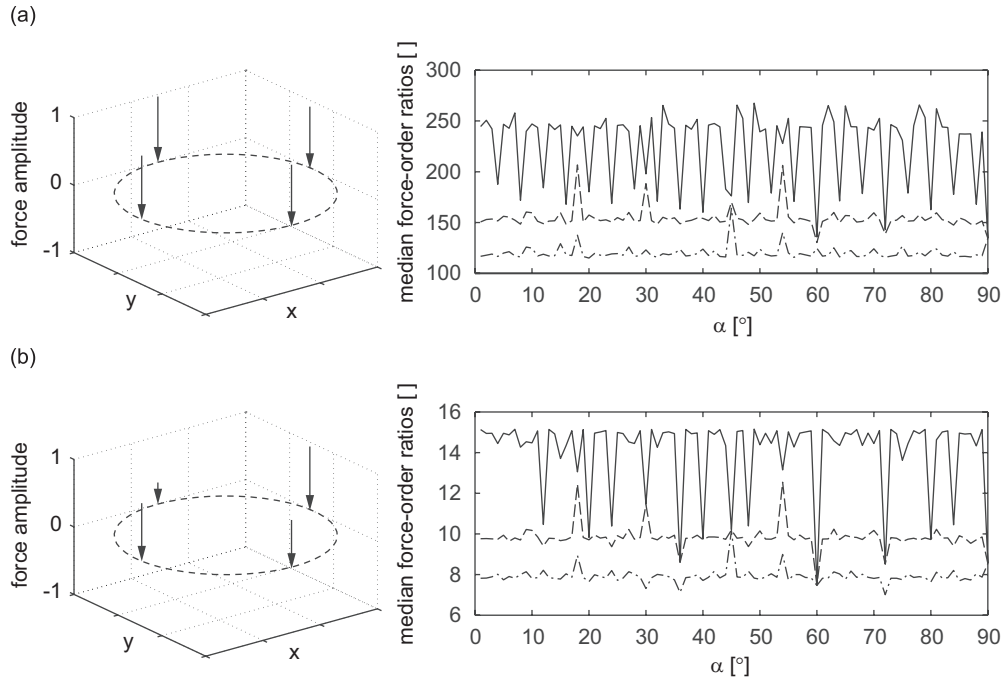

Fig. 14. Median force-order ratios for in-phase contact forces: (a) random magnitude within 0.9–1.0; (b) random magnitude within 0.1–1.0. — 100% confidence interval; – – – 95% confidence interval; – · – 90% confidence interval.

5.2. Deterministic phase of the contact forces

In the mass-controlled region the source structure can be modelled as a rigid body. At frequencies where the relative phases of the contact forces are deterministic at 0 or $\pm\pi$, the two configurations shown in Figs. 3(a) and 4(b) are possible. For the extreme case, where the contact forces have equal magnitude, certain force orders can be equal to zero. In such a case, values of infinity are possible for the force-order ratios. As was observed from measurements of a washing machine and a tumble dryer in Section 4, however, the magnitudes of the contact forces will vary, cf. Ref. [8].

In Fig. 14, results from Monte Carlo simulations are presented for cases of four-point interfaces with in-phase contact forces. The rectangular alignment of the contact points is defined by the angle α, see Fig. 13(a). For every configuration, 100,000 distributions of 100,000 force orders were calculated. If the contact forces are approximately equal in magnitude, the force orders vary by factors larger than 100, see Fig. 14(a). In contrast, a variation of the contact forces of one order of magnitude results in median force-order ratios lower than 10 for the 90% confidence interval, see Fig. 14(b).

For the case that the contact forces have deterministic phase at $\pm\pi$ or 0, respectively, the median force-order ratios for different confidence intervals are plotted in Fig. 15. Here, α describes the angle between two contact forces which are in phase. The results are roughly the same if α is the angle between two out-of-phase contact forces. As for the case where all contact forces are in phase, such as in Fig. 14, a large magnitude range of the force orders is observed if the contact forces are approximately equal in magnitude. Furthermore, a factor 10 in magnitude of the contact forces suffices to lower the median force-order ratios below 10 with a 90% confidence interval.

If the source mechanisms are not coherent, however, the relative phases of the contact forces can assume any value between $\pm\pi$. Inside a washing machine for instance, there are incoherent source mechanisms from the spinning drum and the waterpump. In the mass-controlled region of that source, therefore, the relative phases of the contact forces can be random. As is shown in Table 1 and Fig. 13, much lower force-order ratios can be expected for cases of incoherent source mechanisms.

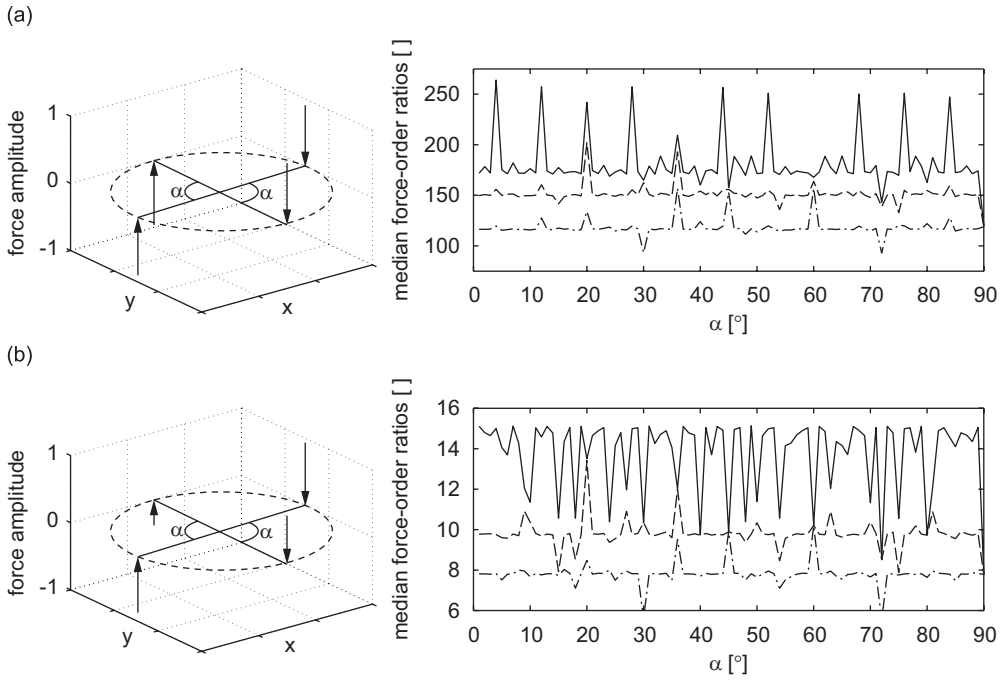

Fig. 15. Median force-order ratios for out-of-phase contact forces: (a) random magnitude within 0.9–1.0; (b) random magnitude within 0.1–1.0. — 100% confidence interval; − − − 95% confidence interval; − · − 90% confidence interval.

6. Concluding remarks

The distribution of force orders depends on the number and location of the contact points as well as on the magnitude and phase of the contact forces. For interfaces with equi-distant spacing between the contact forces, the force orders are grouped according to the number of contact points.

In an experimental investigation of the distribution of force orders, a tumble dryer and a washing machine are analyzed. A uniform concrete floor and a chipboard plate were used as receiving structures. Due to the grouping of the force orders, single orders which dominate or are substantially smaller than all other orders in wide frequency regions do not exist. Furthermore, the magnitudes of all force orders lie within a band with a bandwidth of approximately one order of magnitude. Only at very low frequencies, force-order ratios of up to 100 are observed.

Based on assumptions of the relative magnitudes and phases of the contact forces, results from Monte Carlo simulations are presented. Within the 90% confidence interval, the relative magnitudes of the force orders vary by up to an approximate factor four. Solely at frequencies where the source structure is mass controlled, are observed substantially larger variations. As the mass-controlled region is located at low frequencies [10], these theoretical results are corroborated by those from the measurements.

The comparatively small magnitude range of the force orders at frequencies where the source is not mass controlled suggests that the uniform force-order distribution is a valid approximation. It can furthermore be surmised that the larger range at low frequencies will not fully manifest itself owing to the predominance of the equal-order interface mobility of order zero [2,3]. However, such assumptions are subject to be investigated in conjunction with the complete assessment of the influence of the cross-order terms.

Acknowledgments

The authors gratefully acknowledge the financial support received from the German Research Foundation (DFG) through Grant PE 1155/4-1.

References

[1] J.-M. Mondot, B.A.T. Petersson, Characterization of structure-borne sound sources: the source descriptor and the coupling function, *Journal of Sound and Vibration* 114 (1987) 507–518.
[2] H.A. Bonhoff, B.A.T. Petersson, The influence of cross-order terms in interface mobilities for structure-borne sound source characterization: plate-like structures, *Journal of Sound and Vibration* 311 (2008) 473–484.
[3] H.A. Bonhoff, B.A.T. Petersson, The influence of cross-order terms in interface mobilities for structure-borne sound source characterization: frame-like structures, *Journal of Sound and Vibration* 319 (2009) 305–319.
[4] B.A.T. Petersson, B.M. Gibbs, Use of the source descriptor concept in studies of multi-point and multi-directional vibrational sources, *Journal of Sound and Vibration* 168 (1993) 157–167.
[5] B.A.T. Petersson, An experimental technique for dynamic characteristics at large structural interfaces, *International Congress on Sound and Vibration*, Copenhagen, Denmark, Vol. 6, 1999, pp. 2175–2182.
[6] B.A.T. Petersson, J. Plunt, On effective mobilities in the prediction of structure-borne sound transmission between a source structure and a receiving structure, part 1: theoretical background and basic experimental studies, *Journal of Sound and Vibration* 82 (1982) 517–529.
[7] J.-M. Mondot, Structure-borne sound source characterization, part 3: multi-point installed source structure, Report F86-04, Department of Building Acoustics, Chalmers University of Technology, Göteborg, Sweden, 1986.
[8] H.A. Bonhoff, B.A.T. Petersson, The distribution of force orders on structure-borne sound source interfaces for the concept of interface mobilities, *Proceedings of the Institute of Acoustics* 29 (5) (2007) 74–85.
[9] R.A. Fulford, B.M. Gibbs, Structure-borne sound power and source characterization in multi-point-connected systems, part 1: case studies for assumed force distributions, *Journal of Sound and Vibration* 204 (1997) 659–677.
[10] R.A. Fulford, B.M. Gibbs, Structure-borne sound power and source characterization in multi-point-connected systems, part 2: about mobility functions and free velocities, *Journal of Sound and Vibration* 220 (1999) 203–224.
[11] R.A. Fulford, B.M. Gibbs, Structure-borne sound power and source characterization in multi-point-connected systems, part 3: force ratio estimates, *Journal of Sound and Vibration* 225 (1999) 239–282.
[12] L. Cremer, M. Heckl, B.A.T. Petersson, *Structure-borne Sound*, third ed., Springer, Berlin, 2005.
[13] J.E. Gentle, *Random Number Generation and Monte Carlo Methods*, second ed., Springer, Berlin, 1998.
[14] R.H. Lyon, *Statistical Energy Analysis of Dynamical Systems: Theory and Applications*, MIT Press, Cambridge, MA, 1975.
[15] M.H. DeGroot, M.J. Schervish, *Probability and Statistics*, third ed., Addison-Wesley, Reading, MA, 2002.